LETTER

Hominin occupation of the Chinese Loess Plateau since about 2.1 million years ago

Zhaoyu Zhu[1,2]*, Robin Dennell[3]*, Weiwen Huang[2,4], Yi Wu[5], Shifan Qiu[6], Shixia Yang[4,7], Zhiguo Rao[8], Yamei Hou[2,4], Jiubing Xie[9], Jiangwei Han[10] & Tingping Ouyang[1,11]

Considerable attention has been paid to dating the earliest appearance of hominins outside Africa. The earliest skeletal and artefactual evidence for the genus *Homo* in Asia currently comes from Dmanisi, Georgia, and is dated to approximately 1.77–1.85 million years ago (Ma)[1]. Two incisors that may belong to *Homo erectus* come from Yuanmou, south China, and are dated to 1.7 Ma[2]; the next-oldest evidence is an *H. erectus* cranium from Lantian (Gongwangling)—which has recently been dated to 1.63 Ma[3]— and the earliest hominin fossils from the Sangiran dome in Java, which are dated to about 1.5–1.6 Ma[4]. Artefacts from Majuangou III[5] and Shangshazui[6] in the Nihewan basin, north China, have also been dated to 1.6–1.7 Ma. Here we report an Early Pleistocene and largely continuous artefact sequence from Shangchen, which is a newly discovered Palaeolithic locality of the southern Chinese Loess Plateau, near Gongwangling in Lantian county. The site contains 17 artefact layers that extend from palaeosol S15—dated to approximately 1.26 Ma—to loess L28, which we date to about 2.12 Ma. This discovery implies that hominins left Africa earlier than indicated by the evidence from Dmanisi.

The Lantian area of the Shaanxi province lies on the southern margin of the Chinese Loess Plateau (Fig. 1), which covers about 270,000 square kilometres[7] (Fig. 1). Loess deposition in China since 2.6 Ma has been massive, with up to 100–300 m being deposited on the Loess Plateau[7]. Typical aeolian loess–palaeosol sequences are divided into 33 couplets of alternating palaeosol (S) and loess (L) sediments from top to bottom, from the S0–L1 couplet to the S32–L33 couplet[7,8]. This sequence records East Asian monsoon development since 2.6 Ma and correlates with marine isotope stage 1 to marine isotope stage 102 or 104[9,10]. Loess units correspond to even-numbered marine isotope stages (cold periods or glacial stages) and palaeosol units correspond to odd-numbered marine isotope stages (warm periods or interglacial stages). Numerous sections indicate that Loess Plateau sequences can be correlated over distances of >1,100 km from west to east and >600 km from north to south. Palaeomagnetic dating, which establishes palaeomagnetic reversal boundaries, is the most reliable method for dating these sequences; for example, the Matuyama/Brunhes boundary occurs in the S7–L8 couplet (and sometimes in S8); the Jaramillo subchron between L10 and S12; and the Olduvai subchron in the lower part of L25 to the base of S26[7,8,10–16] (see Supplementary Information). Through palaeomagnetic dating and astronomical tuning[10,14], the age of each loess and palaeosol has been calculated in two schemes to within a precessional cycle (Supplementary Table 1) and used in international correlations of the Quaternary geological timescale[17,18]; here we use the 'Chiloparts' timescale[10] (Supplementary Table 1). Because of questions about the positions of geomagnetic reversals in loess–palaeosol couplets[16,19] and time delays of about 10–30 thousand years for the

recording of polarity reversals in loess[20], we date each unit to within a precessional cycle rather than to the 1-thousand-year precision of the Chiloparts timescale.

The main palaeoanthropological limitation of the Loess Plateau is that it largely lacks evidence of the Early Palaeolithic, or associated hominin remains. The main exception is Lantian county in which a mandible and cranium of *H. erectus* have been found at Chenjiawo and Gongwangling, respectively. Both were dated by palaeomagnetism and correlation with the Luochuan loess–palaeosol sequence[21]. At Chenjiawo the mandible occurs in palaeosol S6 (684–710 thousand years ago), and at Gongwangling the layer containing the cranium is now correlated with S23 (1.59–1.65 Ma)[3]. Although some stone artefacts were found in Lantian county during the 1960s[22,23], they could not be assigned precise geological contexts. A few artefacts have recently been dated to the middle-to-late Pleistocene[24,25].

In our 2004–2017 investigations, we found a new Palaeolithic locality at Shangchen (34° 13′ 33″ N, 109° 28′ 39″ E) about 4 km north of Gongwangling. It is about 74 m thick and complete from L5 to L28 (equivalent to marine isotope stage 12 to marine isotope stage 80) (Fig. 2). After we found artefacts in loess and palaeosol sections, our main aim was to assign these a precise age. Particular attention was paid to evidence of multiple flaking, preferably from more than one direction; the presence of clear flake scars, percussion bulbs, retouch and secondary flake removals to distinguish artefacts from geofacts (Supplementary Information). In some sections, palaeomagnetic samples were taken next to where stone artefacts were discovered to confirm that they were in undisturbed deposits. Stone artefacts and mammalian fossils were also found at the base of S27 and the upper part of L28 in a small excavation in 2017.

Preliminary classifications of loess–palaeosol horizons are based on the identification of marker layers (palaeosol S5 and loess horizons L9, L15, L24 and L25) during our field investigations. Grain-size, chemistry and mineralogy analyses were performed to further distinguish sediment type (Extended Data Fig. 1). These indicate that the strata are aeolian, as are other typical Chinese loess deposits[7,8,10–16]. Rock magnetic measurements indicate that the sediments are suitable for palaeomagnetic dating (Supplementary Information and Extended Data Fig. 2). High-resolution magnetic susceptibility curves, generated from 1,076 samples with an approximately 6.9-cm average sampling interval, show variations that are the same as those of representative Chinese loess sections and confirm our pedostratigraphic identification. Systematic high-resolution palaeomagnetic measurements by progressive thermal demagnetization, based on 722 specimens with an approximately 10-cm average sampling interval, were used to determine the characteristic remanent magnetization direction, after removing one or two soft magnetization components (Extended Data Fig. 3).

[1]Key Laboratory of Ocean and Marginal Sea Geology, Guangzhou Institute of Geochemistry, Chinese Academy of Sciences, Guangzhou, China. [2]State Key Laboratory of Loess and Quaternary Geology, Institute of Earth Environment, Chinese Academy of Sciences, Xi'an, China. [3]Department of Archaeology, University of Exeter, Exeter, UK. [4]Key Laboratory of Vertebrate Evolution and Human Origins, Institute of Vertebrate Paleontology and Paleoanthropology, Chinese Academy of Sciences, Beijing, China. [5]Key Laboratory of Ocean and Marginal Sea Geology, South China Sea Institute of Oceanology, Chinese Academy of Sciences, Guangzhou, China. [6]School of Geography and Environmental Engineering, Gannan Normal University, Ganzhou, China. [7]State Key Laboratory of Lithospheric Evolution, Institute of Geology and Geophysics, Chinese Academy of Sciences, Beijing, China. [8]College of Resources and Environmental Sciences, Hunan Normal University, Changsha, China. [9]Environmental Supervision Detachment of Nanning, Nanning, China. [10]Henan Institute of Geological Survey, Zhengzhou, China. [11]School of Geography, South China Normal University, Guangzhou, China. *e-mail: zhuzy@gig.ac.cn; r.w.dennell@exeter.ac.uk
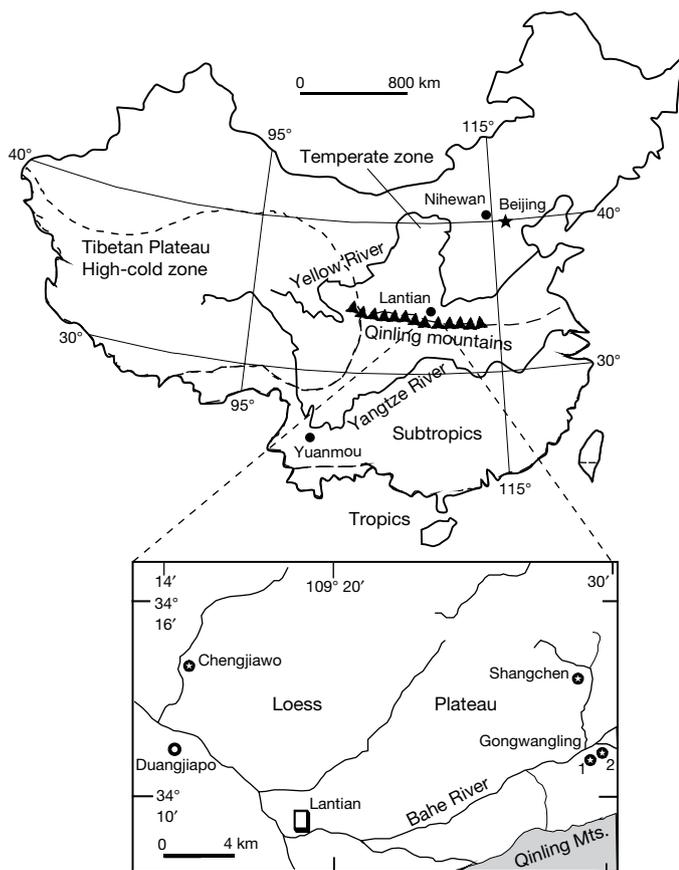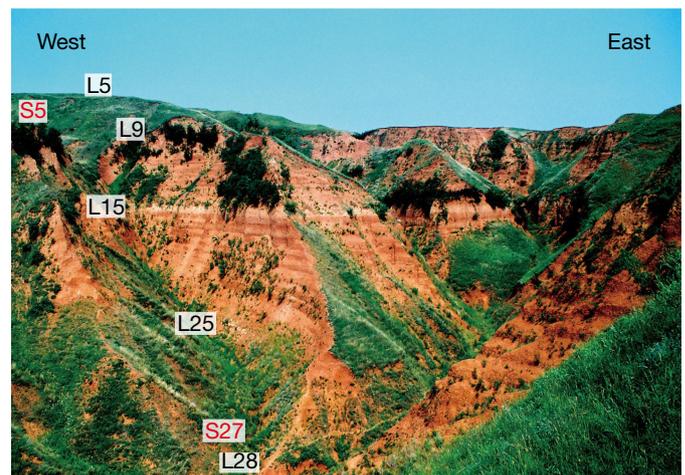
Fig. 2 | The landscape and loess–palaeosol section of the Shangchen Palaeolithic locality. The steep and dissected terrain exposes an aeolian loess–palaeosol sequence from L5 (412–479 thousand years ago) to L28 (2.11–2.13 Ma) that is fully developed, particularly with marker horizons such as the tripartite S5 with the reddest colour and highest magnetic susceptibility or the units L9 (869–943 thousand years ago), L15 (1.24–1.26 Ma) and L24–L25 (1.65–1.80 Ma), which represent particularly thick and silty loess (with coarse grain size) with a notable yellowish-white colour and lowest magnetic susceptibility. On the basis of these marker horizons, palaeomagnetic sampling and artefact collecting have been divided into five subsections along the continuously developed gully, and the main stratigraphic sequence has been established (see Supplementary Information and Extended Data Figs. 4, 5 for details). Many artefacts have been found in situ within the sampled area.

Fig. 1 | Location map of the Chinese Loess Plateau and the Lantian area. The Qinling Mountains form the climatic and biological boundary between the temperate north and subtropical south of China. The locations of major hominin sites in China, including the Nihewan basin and Yuanmou, are indicated. The Lantian basin lies in the southern Loess Plateau and north of the Qinling Mountains in the temperate zone of north China with Palaeolithic localities such as Gongwangling, Chenjiawo and Shangchen in the Lantian area. The main section of Shangchen is situated on denudated loess tablelands at an altitude of 898 m, along the north bank of the Bahe River. Duanjiapo is one of the typical sections of the Chinese loess–palaeosol sequence. Localities marked as 1 and 2 refer to Gongwangling 1 and Gongwangling 2, respectively.

The magnetic polarity for each specimen was used to establish the local magnetostratigraphy (see Fig. 3, Supplementary Information, Extended Data Figs. 4, 5 and Source Data), and from this precise ages have been assigned to the artefacts in the loess–palaeosol sequence.

Eight major magnetozones are recorded in the Shangchen section (Fig. 3), four of which have normal polarity (N1 to N4) and four of which have reversed polarity (R1 to R4). By comparison with the geomagnetic polarity timescale[26,27], magnetozone N1 corresponds to the Brunhes chron, and the Matuyama/Brunhes boundary (0.78 Ma) is in horizons S7 to L8; magnetozone N2 corresponds to the Jaramillo subchron (0.99–1.07 Ma) and lies between horizons S10 and S12; magnetozone N3 corresponds to the Olduvai subchron (1.78–1.95 Ma), with its top and base lying within the lower part of L25 and the base of S26, respectively; and magnetozone N4 corresponds to the Réunion excursion (2.13–2.15 Ma) in L28. The four reversed polarity magnetozones are attributed to different periods of the Matuyama chron. A short-term polarity event, labelled e₁, might correspond to the Punaruu excursion at about 1.12 Ma[28] (see Supplementary Information). Stratigraphic continuity and the position of reversal boundaries in the Shangchen section indicate that the loess–palaeosol sequence is complete from L5 to L28 through a date range of approximately 0.41–2.16 Ma[10,27]. By using marker layers and palaeomagnetic reversal boundaries of offset sections[29] (see Supplementary Information and Extended Data Figs. 4, 5),

the comprehensive main section and timescale of the Shangchen locality have been established from five subsections.

At Shangchen, 88 flaked and 20 unmodified stones were found in situ between S5 and L28. Here we discuss only those found in situ ($n = 96$) in layers S15 to L28, which date from 1.26 Ma to 2.12 Ma. The 82 flaked and 14 unmodified stones between S15 and L28 (Supplementary Table 6) were collected from 6 loess and 11 palaeosol strata within trenches cut for palaeomagnetic sampling, in situ at distances of less than 100 m from these trenches and exposed in the surfaces of 50–80° slopes, or within a 15.4-m² excavated area of S27–L28 (see Supplementary Information and Extended Data Figs. 6–10). Five categories of flaked stone were recognized: cores (17), flakes (9), flake fragments (8), fragments (14) and retouched pieces (34). The 34 retouched items were classified as scrapers (17), notches (4), scraper and/or notches (4), points and/or borers (6) and picks and/or bifaces (3). Cores were produced by bipolar ($n = 2$) and hard hammer percussion ($n = 15$), and those on elongate cobbles ($n = 9$) were most common. The average number of flakes per core was 4.6 (range of 1–7), from a mean of 2.3 directions (range of 1–6). As no natural stone exposures (for example, stream beds or outcrops) were encountered, isolated unmodified cobbles are regarded as manuports that may have been intended as cores or used as hammerstones. Two pieces identified as hammerstones show percussion damage. All artefacts except one were fresh, with no sign of rolling or abrasion. The most common raw materials (Supplementary Table 6) are different types of quartzite ($n = 72$) and quartz ($n = 20$) and their probable source is the foothills of the Qinling Mountains—which are situated 5–10 km to the south of the site—and the streams flowing from them. The horizon with the most stone items is S22 ($n = 33$, 1.54–1.57 Ma) (Supplementary Table 8 and Extended Data Fig. 6). A total of 28 stones (25 flaked and 3 unmodified) were found below S22 (Fig. 4). In S23 (1.59–1.65 Ma) a flake and a flake fragment were found; in S24 (1.71–1.73 Ma), a notch, scraper, core and two flake fragments; in L25 (1.73–1.80 Ma), a scraper, hammerstone, and two fragments; in S26 (1.89–1.95 Ma), a cobble; in L27 (1.95–2.09 Ma), a cobble and a fragment; and in S27 (2.09–2.12 Ma) (Extended Data Fig. 7), six artefacts were found (three cores, a core
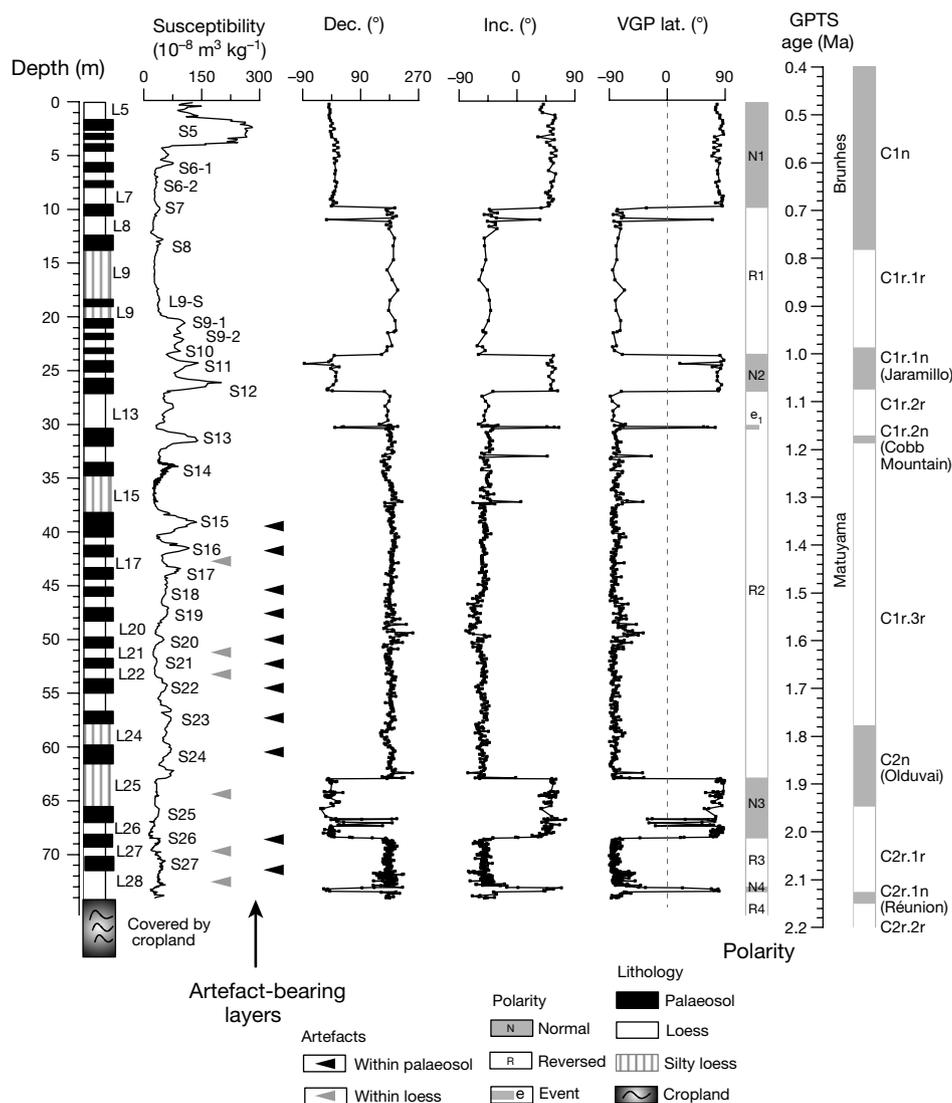
Fig. 3 | Summary of the loess–palaeosol section with artefact sequence of the Shangchen Palaeolithic locality. Magnetic susceptibility variations (high values in palaeosols and low values in loess), and the positions of key marker layers (S5, L9, L15 and L24–L25) are the same as in the standard Loess Plateau sections[7,8,10–16]. The geomagnetic polarity timescale is from previous publications[26,27]. Details of the palaeomagnetic data and artefacts within 17 excavation layers (S15, S16, S18–S24, S26 and S27, and L17, L21, L22, L25, L27 and L28) are provided in Supplementary Information, Extended Data Figs. 5–10 and Source Data. Artefacts found above S15 are not included in this paper because here we focus on the artefacts earlier than about 1.2 Ma. There are four normal polarity magnetozones, comprising N1 (chron C1n, 0–9.71 m), N2 (C1r.1n, 23.50–26.90 m), N3 (C2n, 62.94–68.44 m) and N4 (C2r.1n, 73.08–73.41 m). Four reversed polarity magnetozones, comprising R1 (9.71–23.50 m), R2 (26.90–62.94 m), R3 (68.44–73.08 m) and R4 (73.41–74.05 m), are attributed to different periods of the Matuyama chron. In addition, as an independent check on the Chiloparts timescale, we have estimated the ages of the main layers by using the average sedimentation rate of each segment to obtain the sedimentation rate age (see Supplementary Tables 2–5). The age difference between our sedimentation rate age and the Chiloparts timescale is small (~2.16%) and we therefore use the internationally recognized Chiloparts timescale throughout this paper. Dec., declination; GPTS, geomagnetic polarity timescale; Inc., inclination; VGP, virtual geomagnetic pole.

and/or scraper, a pointed piece and a flake tool). In the excavation into S27 and L28 (Extended Data Figs. 8, 9), a core and a flake tool were found at the S27/L28 boundary, and six artefacts were found in L28 (approximately 2.12 Ma): three scrapers, a point, a pointed piece and a flake. A mandibular fragment of a cervid, a bovid and other fossil bone fragments were also found (Extended Data Fig. 10). Using the Chiloparts timescale, the stone artefact and fossil horizon in the upper part of L28 between the Olduvai subchron and the Réunion excursion is dated to about 2.12 Ma. Details of artefact features are indicated in Supplementary Tables 6–8. Images of artefacts being extracted from original strata are shown in Extended Data Figs. 6–9, and laser three-dimensional scans of three pieces are shown in Supplementary Videos 1–3. All artefacts in these figures have clear flake features and evidence of repeated flaking from more than one direction. They are also consistent with the rest of the artefact sequence from Shangchen

with respect to raw materials, flaking techniques and type of flaking product.

Four aspects of our discoveries at the Shangchen Palaeolithic locality are noteworthy. First, we have for the first time—to our knowledge—established the age of Early Pleistocene (below L15) artefacts in the Loess Plateau within a rigorous stratigraphic framework. Second, stone artefacts were found predominantly in 11 palaeosol layers (S15, S16, S18–S24, S26 and S27, with 80 items), which developed in a warm and wet climate, but in only 6 loess layers (L17, L21, L22, L25, L27 and L28, with 16 items), which indicate colder and drier conditions (Fig. 3). This pattern is consistent with that found in the loess–palaeosol sequence in Tajikistan[30]. Third, the 17 loess–palaeosol layers with artefacts span about 0.85 million years and indicate repeated—but not necessarily continuous—hominin occupation of the Chinese Loess Plateau between 1.26 and 2.12 Ma, equivalent to marine isotope stage
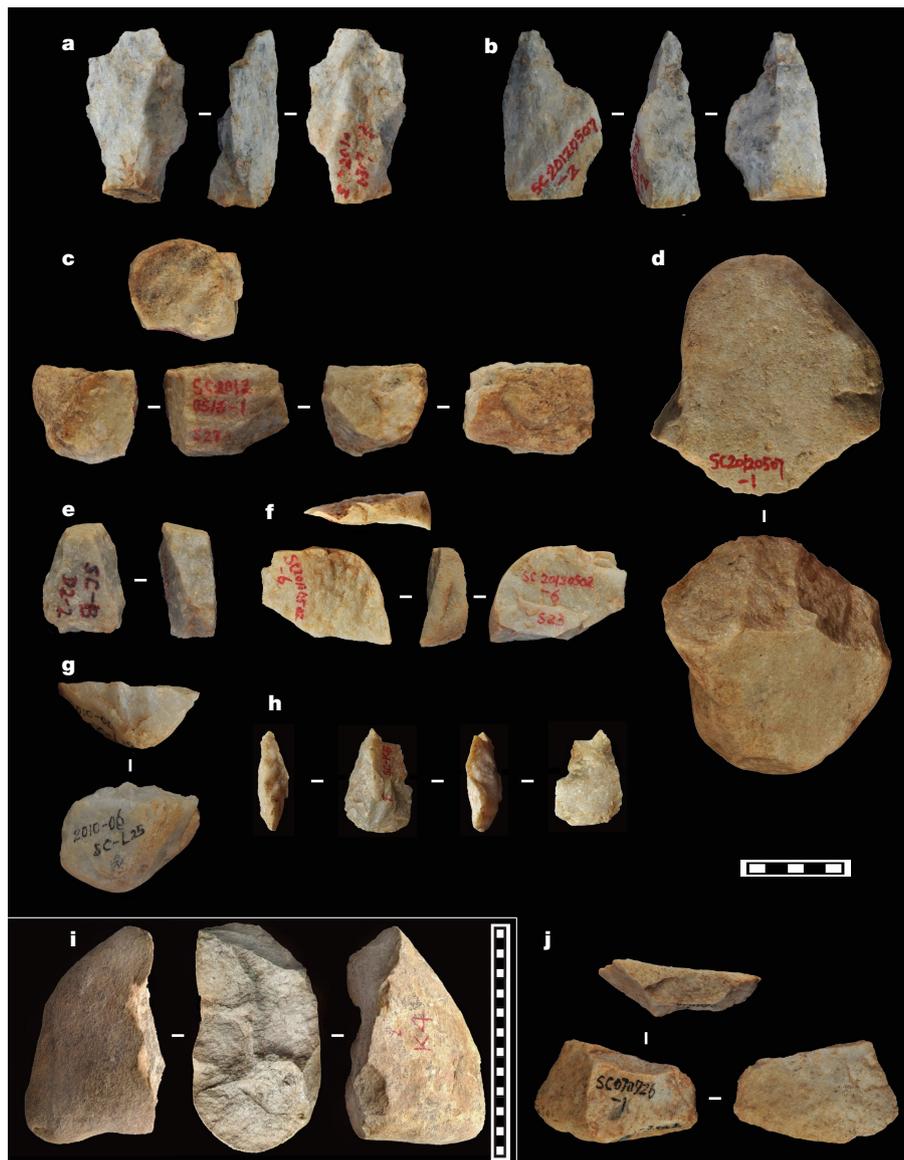
Fig. 4 | Selected artefacts found in situ in layers S27–L28 (2.09–2.12 Ma), L27 (1.95–2.09 Ma), L25 (1.73–1.80 Ma) and S23 (1.59–1.65 Ma) from the Shangchen Palaeolithic locality. a, SC 20120507-3, a flake tool from S27. **b**, SC 20120507-2, a pointed piece from S27. **c**, SC 20120516-1, a core from S27. **d**, SC 20120507-1, a core from S27. **e**, SC-B D2-2, a bipolar fragment from L27. **f**, SC 20120502-6, a flake from S23. **g**, 2010-06 SC-L25, a scraper from L25. **h**, SC-K5, a flake tool from S27–L28. **i**, SC-K4, a core from S27–L28. **j**, SC070926-1, a flake fragment from S23. Artefacts from S23 are similar in age to the the Gongwangling *H. erectus* cranium[3]. Each gradation in the scales represents 1 cm. Artefacts SC-K4 and SC-K5 are also shown in Extended Data Fig. 10. SC, abbreviation for Shangchen site.

39 to marine isotope stage 80. Fourth, and most importantly, the oldest artefact age of approximately 2.12 Ma at Shangchen implies that hominins had left Africa before the date suggested by the earliest evidence from Dmanisi (about 1.85 Ma). This makes it necessary to reconsider the timing of initial dispersal of early hominins in the Old World.

Data availability
The authors declare that all data supporting the findings of this study are available within the paper and its Supplementary Information. Source Data for Fig. 3 are provided with the paper.

Online content
Any Methods, including any statements of data availability and Nature Research reporting summaries, along with any additional references and Source Data files, are available in the online version of the paper at https://doi.org/10.1038/s41586-018-0299-4.

1. Ferring, R. et al. Earliest human occupations at Dmanisi (Georgian Caucasus) dated to 1.85–1.78 Ma. *Proc. Natl Acad. Sci. USA* **108**, 10432–10436 (2011).
2. Zhu, R. X. et al. Early evidence of the genus *Homo* in East Asia. *J. Hum. Evol.* **55**, 1075–1085 (2008).
3. Zhu, Z. Y. et al. New dating of the *Homo erectus* cranium from Lantian (Gongwangling), China. *J. Hum. Evol.* **78**, 144–157 (2015).
4. Zaim, Y. et al. New 1.5 million-year-old *Homo erectus* maxilla from Sangiran (Central Java, Indonesia). *J. Hum. Evol.* **61**, 363–376 (2011).
5. Zhu, R. X. et al. New evidence on the earliest human presence at high northern latitudes in northeast Asia. *Nature* **431**, 559–562 (2004).
6. Ao, H., Dekkers, M. J., Wei, Q., Qiang, X. & Xiao, G. New evidence for early presence of hominids in North China. *Sci. Rep.* **3**, 2403 (2013).
7. Liu, T. S. et al. *Loess and the Environment* (China Ocean, Beijing, 1985).
8. Rutter, N., Ding, Z., Evans, M. E. & Liu, T. Baoji-type pedostratigraphic section, Loess Plateau, north-central China. *Quat. Sci. Rev.* **10**, 1–22 (1991).
9. Lisiecki, L. E. & Raymo, M. E. A Pliocene-Pleistocene stack of 57 globally distributed benthic $\delta^{18}O$ records. *Paleoceanography* **20**, PA1003 (2005).
10. Ding, Z. L. et al. Stacked 2.6-Ma grain size record from the Chinese loess based on five sections and correlation with the deep-sea ^{18}O record. *Paleoceanography* **17**, 5-1–5-21 (2002).
11. Heller, F. & Liu, T.-S. Magnetostratigraphical dating of loess deposits in China. *Nature* **300**, 431–433 (1982).

12. Kukla, G. & An, Z. Loess stratigraphy in central China. *Palaeogeogr. Palaeoclimatol. Palaeoecol.* **72**, 203–225 (1989).
13. Zheng, H., An, Z. & Shaw, J. New contributions to Chinese Plio-Pleistocene magnetostratigraphy. *Phys. Earth Planet. Inter.* **70**, 146–153 (1992).
14. Heslop, D., Langereis, C. G. & Dekkers, M. J. A new astronomical timescale for the loess deposits of Northern China. *Earth Planet. Sci. Lett.* **184**, 125–139 (2000).
15. Guo, Z. T., Jiang, W. Y., Lu, H. Y., Wu, N. Q. & Yao, X. F. Pleistocene climate extremes in East Asia and their causes. *Earth Sci. Frontiers* **9**, 113–120 (2002).
16. Liu, Q., Roberts, A. P., Rohling, E. J., Zhu, R. & Sun, Y. Post-depositional remanent magnetization lock-in and the location of the Matuyama–Brunhes geomagnetic reversal boundary in marine and Chinese loess sequences. *Earth Planet. Sci. Lett.* **275**, 102–110 (2008).
17. Gibbard, P. & Cohen, K. M. Global chronostratigraphical correlation table for the last 2.7 million years. *Episodes* **31**, 243–247 (2008).
18. Cohen, K. M. & Gibbard, P. L. Global chronostratigraphical correlation table for the last 2.7 million years. http://www.stratigraphy.org/index.php/ics-chart-timescale (2016).
19. Liu, Q. et al. Magnetostratigraphy of Chinese loess–paleosol sequences. *Earth Sci. Rev.* **150**, 139–167 (2015).
20. Sun, Y., Clemens, S. C., An, Z. & Yu, Z. Astronomical timescale and palaeoclimatic implication of stacked 3.6-Myr monsoon records from the Chinese Loess Plateau. *Quat. Sci. Rev.* **25**, 33–48 (2006).
21. An, Z. & Ho, C. New magnetostratigraphic dates of Lantian *Homo erectus*. *Quat. Res.* **32**, 213–221 (1989).
22. Dai, E.-J. & Chi, H.-G. Discovery of palaeoliths at Lantian, Shensi. *Vertebrata PalAsiatica* **8**, 152–156, 161 (1964).
23. Tai, E. C. & Hsu, C. H. New finds of palaeoliths from Lantian. *Acta Archaeologica Sinica* **1**, 1–12 (1973).
24. Wang, S. et al. Newly discovered Palaeolithic artefacts from loess deposits and their ages in Lantian, central China. *Chin. Sci. Bull.* **59**, 651–661 (2014).
25. Zhuo, H. X. et al. Chronology of newly-discovered paleolithic artifact assemblages in Lantian (Shaanxi province), central China. *Quat. Res.* **86**, 316–325 (2016).
26. Cande, S. C. & Kent, D. V. Revised calibration of the geomagnetic polarity timescale for the Late Cretaceous and Cenozoic. *J. Geophys. Res.* **100**, 6093–6095 (1995).
27. Ogg, J. G. in *The Geologic Time Scale 2012* (eds Gradstein, F. M. et al.) 85–114 (Elsevier, Oxford, 2012).
28. Roberts, A. P. Geomagnetic excursions: knowns and unknowns. *Geophys. Res. Lett.* **35**, L17307 (2008).
29. Kappelman, J. et al. in *Geology and Paleontology of the Miocene Sinap Formation, Turkey* (eds Fortelius, M. et al.) 41–66 (Columbia Univ. Press, New York, 2003).
30. Ranov, V. The 'loessic palaeolithic' in South Tadjikistan, central Asia: its industries, chronology and correlation. *Quat. Sci. Rev.* **14**, 731–745 (1995).

Extended Data Fig. 1 | Material composition of aeolian deposits in the Lantian area. a, **b**, Grain size distributions for loess (**a**) and palaeosol (**b**) samples from the Shangchen section. The features of sediments in Shangchen section are the same as those from the Lingtai section[31], which is one of the typical Chinese loess sections. This indicates that sediments from the Shangchen section are aeolian deposits that are similar to those at Lingtai. **c**, Comparison of major elements between the loess sediments at Lantian and Luochuan[7]. The *x* and *y* coordinates represent logarithmic values of the major element content of loess from Luochuan and Lantian, respectively, and the plot shows that loess from the two sites is geochemically similar (data fall on or close to the 1:1 line). **d**, Chondrite-normalized rare-earth element distribution patterns for loess and palaeosol samples from the Shangchen section. Characteristics of partition modes of rare-earth elements from loess and palaeosol samples in the Shangchen section indicate they are the same as those from the Luochuan section.

31. Sun, Y. B., Lu, H. Y. & An, Z. S. Grain size distribution of quartz isolated from Chinese loess/paleosol. *Chin. Sci. Bull.* **45**, 2296–2298 (2000).
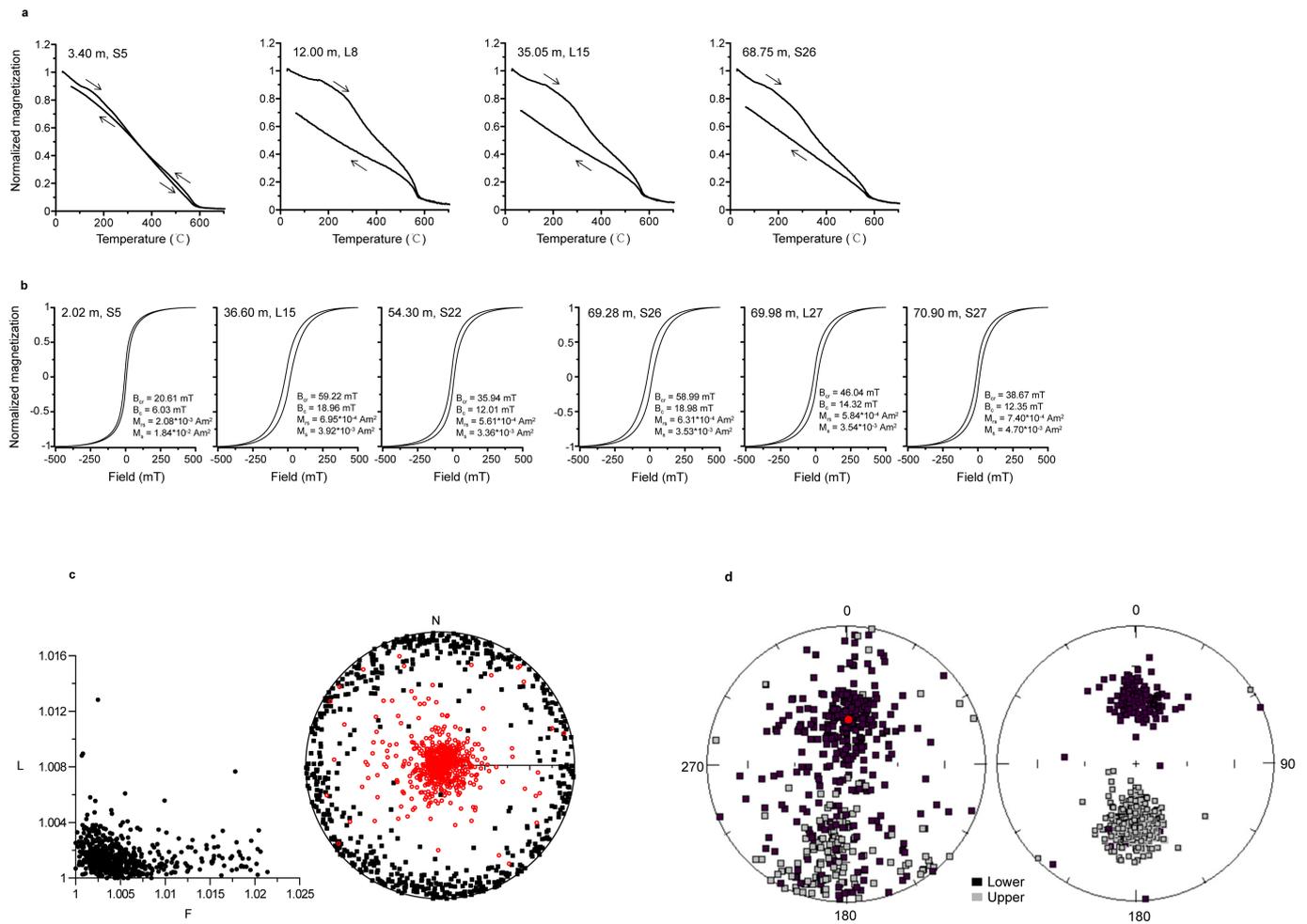
Extended Data Fig. 2 | Rock magnetism. a, Temperature-dependent magnetization variations for four representative samples from the Shangchen section. Arrows indicate heating or cooling runs. These curves were obtained in air using a field of 100 mT, and indicate the presence of maghemite, dominant magnetite and haematite. This type of magnetic mineral assemblage is typical of that previously recovered for the Chinese loess–palaeosol sequence[19,32]. **b**, Hysteresis loops for representative samples after correction for paramagnetic slope. M_s, saturation magnetization; M_{rs}, saturation remanence; B_c, coercive force; and B_{cr}, coercivity of remanence. **c**, Anisotropy of magnetic susceptibility for 694

specimens from loess L5 to loess L28 in the main section that we studied, and parallel sections at the Shangchen locality. Left, Flinn diagram. L, lineation ($\kappa_{max}/\kappa_{int}$). F, foliation ($\kappa_{int}/\kappa_{min}$). Right, stereographic projections of anisotropy-of-magnetic-susceptibility ellipsoids of specimens. Data for κ_{max} and κ_{min} are shown as black squares and red circles, respectively. The data are indicative of normal, undisturbed sedimentary fabrics and support the magnetostratigraphic interpretation presented in this study. **d**, Equal area projections for the natural remanent (left) and characteristic remanent (right) magnetization directions for all 694 studied specimens.

32. Liu, Q., Deng, C., Torrent, J. & Zhu, R. Review of recent developments in mineral magnetism of Chinese loess. *Quat. Sci. Rev.* **26**, 368–385 (2007).
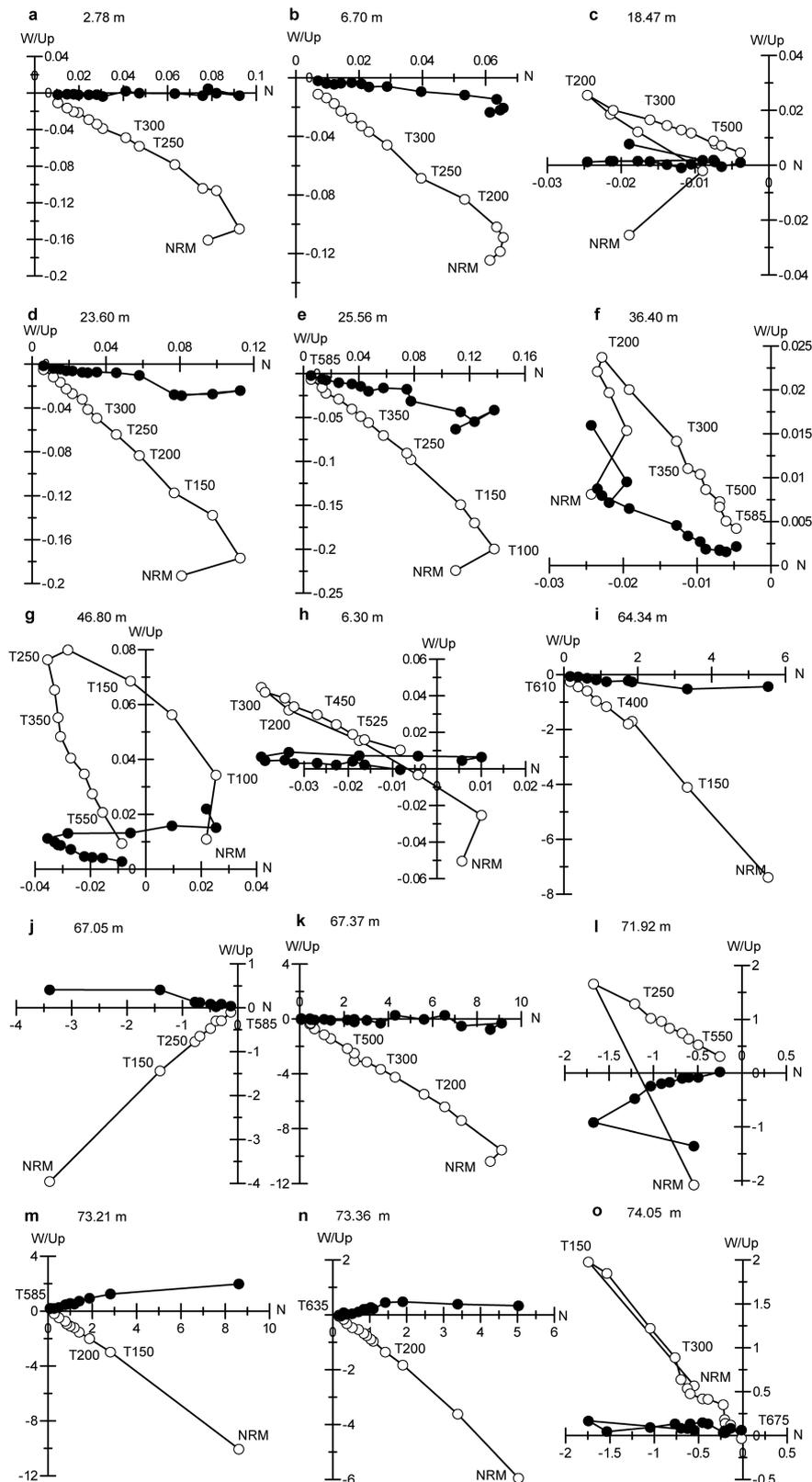
Extended Data Fig. 3 | Palaeomagnetic dating. a–o, Demagnetization diagrams for representative specimens from the Shangchen section. Solid and open symbols refer to data projected onto the horizontal and vertical planes, respectively. Scales of demagnetization temperature and coordinate axes are in degrees Celsius and mA m^{-1}, respectively. In **m**, **n**, the specimens from the magnetic horizon of the Réunion excursion are shown. See Source Data for detailed listings of palaeomagnetic data from the Shangchen section.
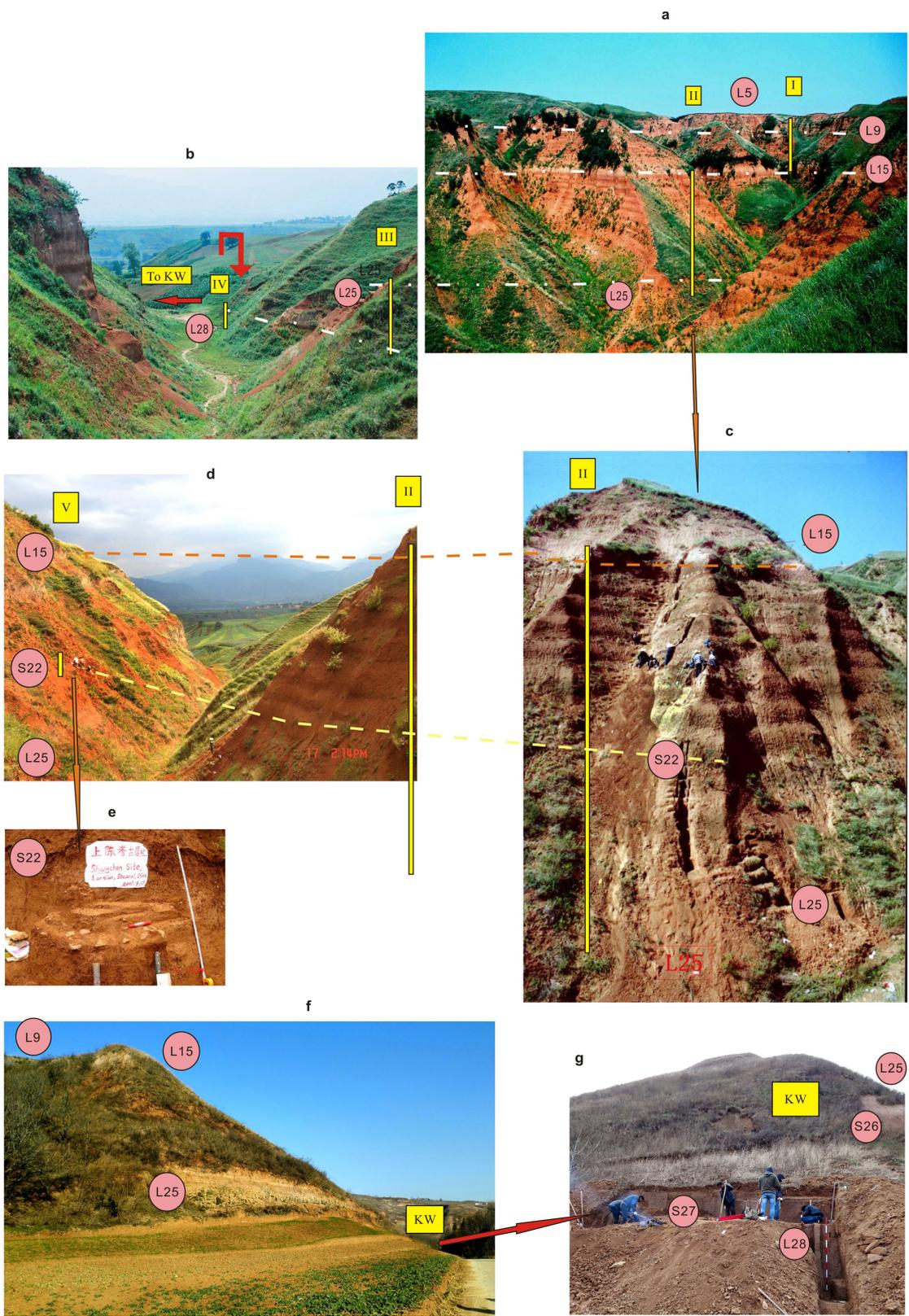
Extended Data Fig. 4 | See next page for caption.

**Extended Data Fig. 4 | Landscape in which palaeomagnetic sampling and artefact collecting were carried out at the Shangchen locality.** The establishment of magnetostratigraphy in the Shangchen locality was based on the traditional and effective-linking methods (using marker layers and palaeomagnetic reversal boundaries of offset sections[29]). The comprehensive main section and timescale of the Shangchen locality have been established from five subsections, the spatial distribution of which is shown below. **a**, **b**, The main sections are exposed continuously along the same gully. Because of the steep terrain and multistep gully bottom (see **c**, **d**), we divided the sampling into four subsections (offset sections) in this gully. Several marker layers—such as L9, L15 and L25—that are white and thick are obvious in the section at short range and can easily be used to link the subsections. The subsections I, II, III and IV contain the following layers: I (L5–L15), II (L15–L25), III (L25–L27), and IV (L27-L28, on the other side of the slope). **c**, The steep subsection II with fresh outcrops of original loess and palaeosols. Many artefacts were found within more than 10 horizons in subsection II or on both its sides. The first artefact was found here in S22. Note the two individuals on the upper part of the section as an approximate scale. **d**, Subsection V, which is a short parallel section opposite subsection II (**c**). **e**, Many artefacts were found in situ in palaeosol S22 during our sampling and excavation. Palaeomagnetic analysis confirms that the artefacts were collected from undisturbed loess or palaeosol (see Supplementary Information). The steepness of slope (shown in **c**, **d**) prevents large-scale excavation. More details can be seen in Extended Data Fig. 6. **f**, **g**, The section of the exploratory trench (named subsection KW) contains layers L25–L28. It is part of the same small hill as the main composite section (subsections I–IV), and is located about 500 m northeast of palaeomagnetic section IV (see Extended Data Fig. 5a). Based on the outcrops of marker layers L9, L15 and L25 in the loess–palaeosol sequence, these sections can easily be linked (see Extended Data Fig. 5 for further details).
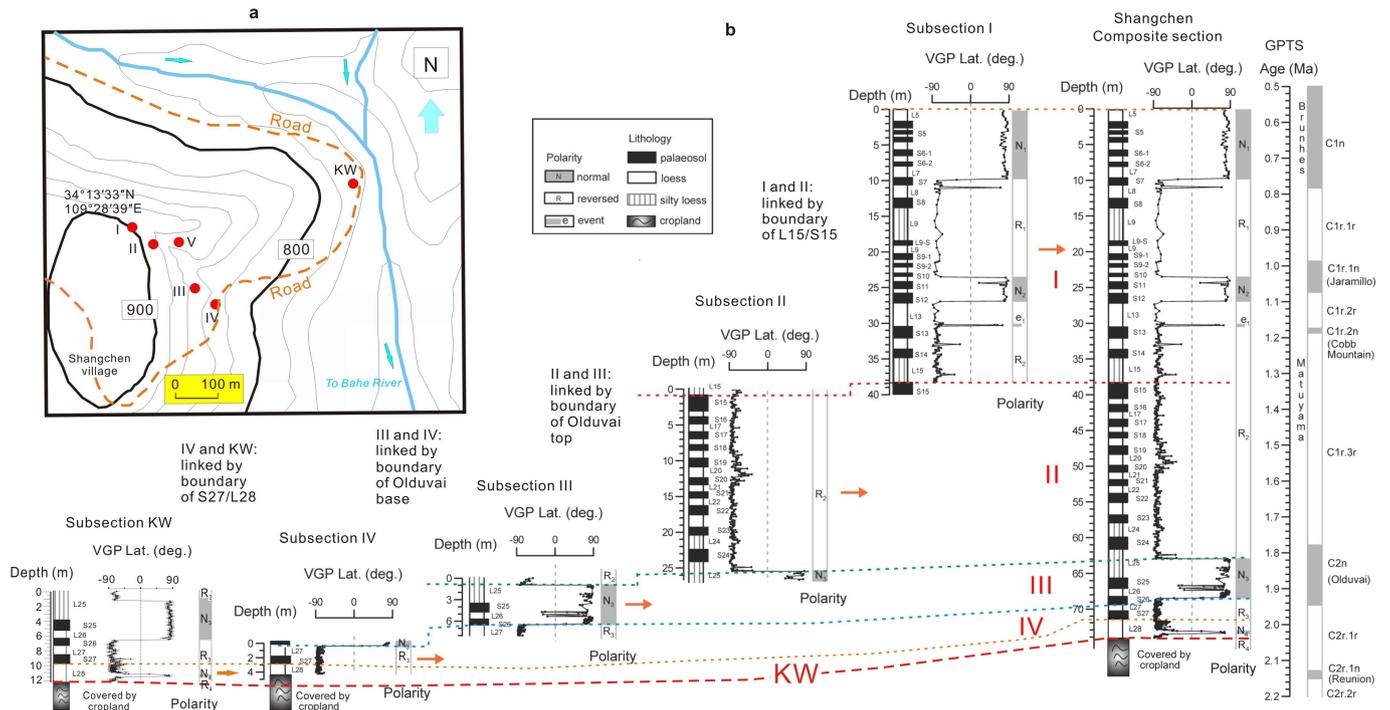
Extended Data Fig. 5 | Distribution and linking method of sections at the Shangchen locality. a, Schematic plan of the subsections of palaeomagnetic sampling. The numbers 800 and 900 refer to the height in metres above sea level. The contour interval is 20 m. Subsection KW refers to the additional parallel section from L25 to L28 with the excavation into S27 and L28. **b**, Schematic of the method used to link the five subsections in the Shangchen locality. This figure and Extended Data Fig. 4 show the loess–palaeosol stratigraphy, with key marker layers, sampled subsections and the locations where artefacts were found. The details of the method used to link the five subsections are given below. Subsections I and II are linked on the basis of the L15/S15 boundary. Measured horizons of subsection I start from the mid-to-lower part of L5 and run downward to the base of marker layer L15 (to the boundary of L15/S15). Measured horizons of subsection II start from the lowest part of L15 and run downward to the lower part of L25. Because the measured thickness of marker layer L15 is the same in both subsections I and II, we cut out the overlapped L15 in subsection II. Thus, subsection I ends at the base of L15, and subsection II begins at the top of S15. Subsections II and III are linked on the basis of the top boundary of the Olduvai subchron. A small normal-polarity segment of the Olduvai subchron was detected in the marker layer L25 at the base of II. Measured horizons of subsection III start from the lower part of L25 to the top of L27, and record the entire Olduvai subchron with a small reversed-polarity segment on the top (in L25) and at the base (top of L27) of the subsection. Thus, the overlapped normal-polarity segment of the Olduvai subchron at the base of subsection

II and a small reverse-polarity segment on top of subsection III were cut out. The reverse-polarity segment at the base of subsection II is linked to the normal-polarity top segment of subsection III, and the whole normal-polarity segment of the Olduvai subchron is contained within subsection III. Subsections III and IV were linked on the basis of the base of the Olduvai subchron. Measured horizons of subsection IV start from the top of L27 to the mid-to-upper part of L28, with a small normal-polarity segment of the base of the Olduvai subchron at the top. After cutting out both the small reverse-polarity segment at the base of subsection III and the small normal-polarity segment on top of subsection IV, the reverse-polarity segment just below the Olduvai subchron in subsection IV is linked to the normal-polarity base of the Olduvai segment in subsection III. Subsection KW contains horizons of L25 (marker layer) to L28, including units L25, S25, L26, S26, L27, S27 and L28. Against the general background of reversed magnetostratigraphy, two normal magnetozones— the Olduvai subchron (1.78–1.95 Ma) and the Réunion excursion (2.13–2.15 Ma)—are recorded. Therefore, section IV and section KW are linked by the base of S27 (that is, S27 at the base of section IV is linked to L28 at the top of subsection KW). Subsection V is opposite of subsection II, which is on the other side of a narrow gully and has two distinct marker layers, L15 in the upper half and L25 in the lower half. There is a palaeosol layer with many artefacts in the middle part of subsection V. The stratigraphic correlation and horizon number demonstrate that this layer belongs to S22. Palaeomagnetic measurements on samples collected from this parallel section all showed reversed polarity.
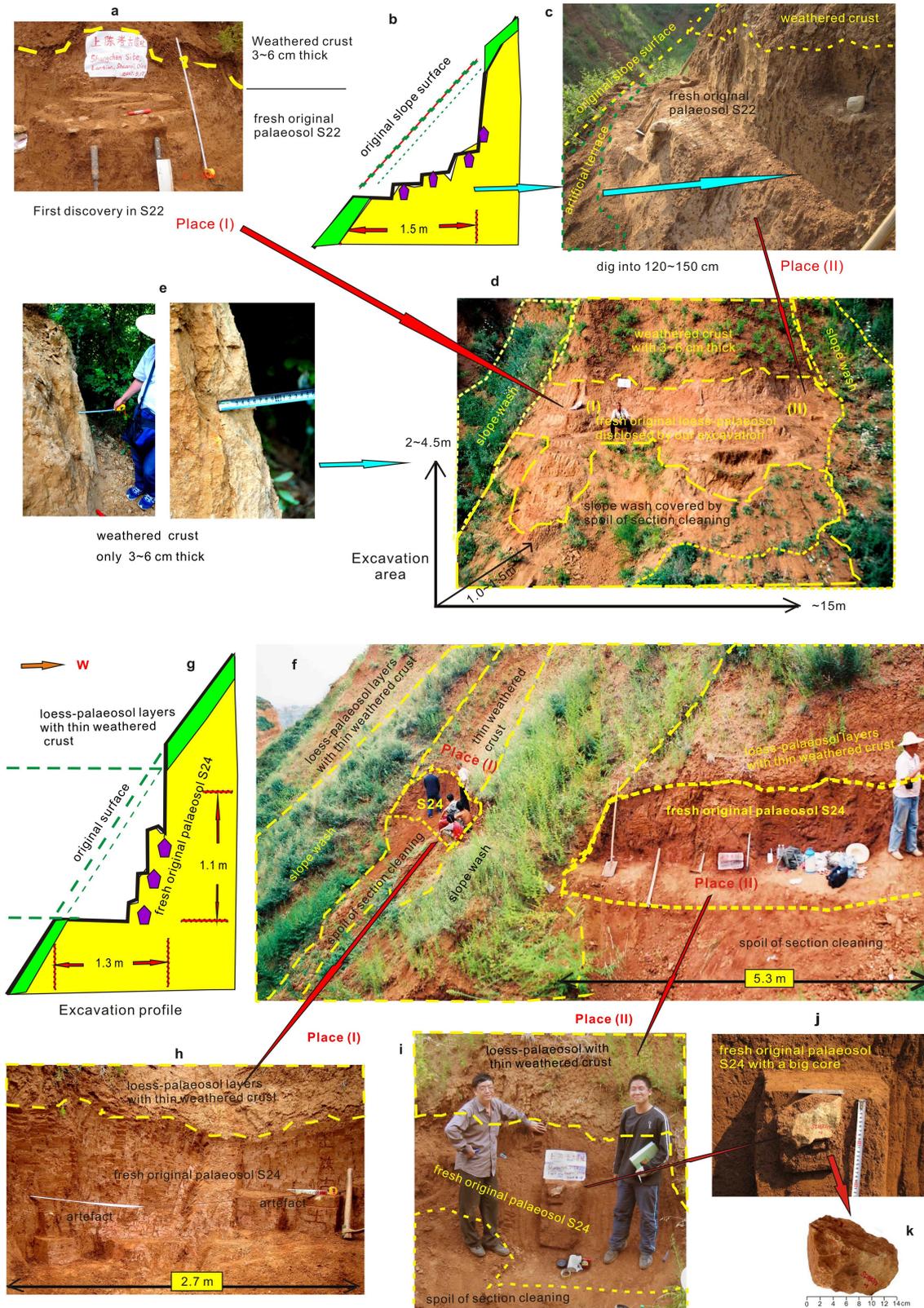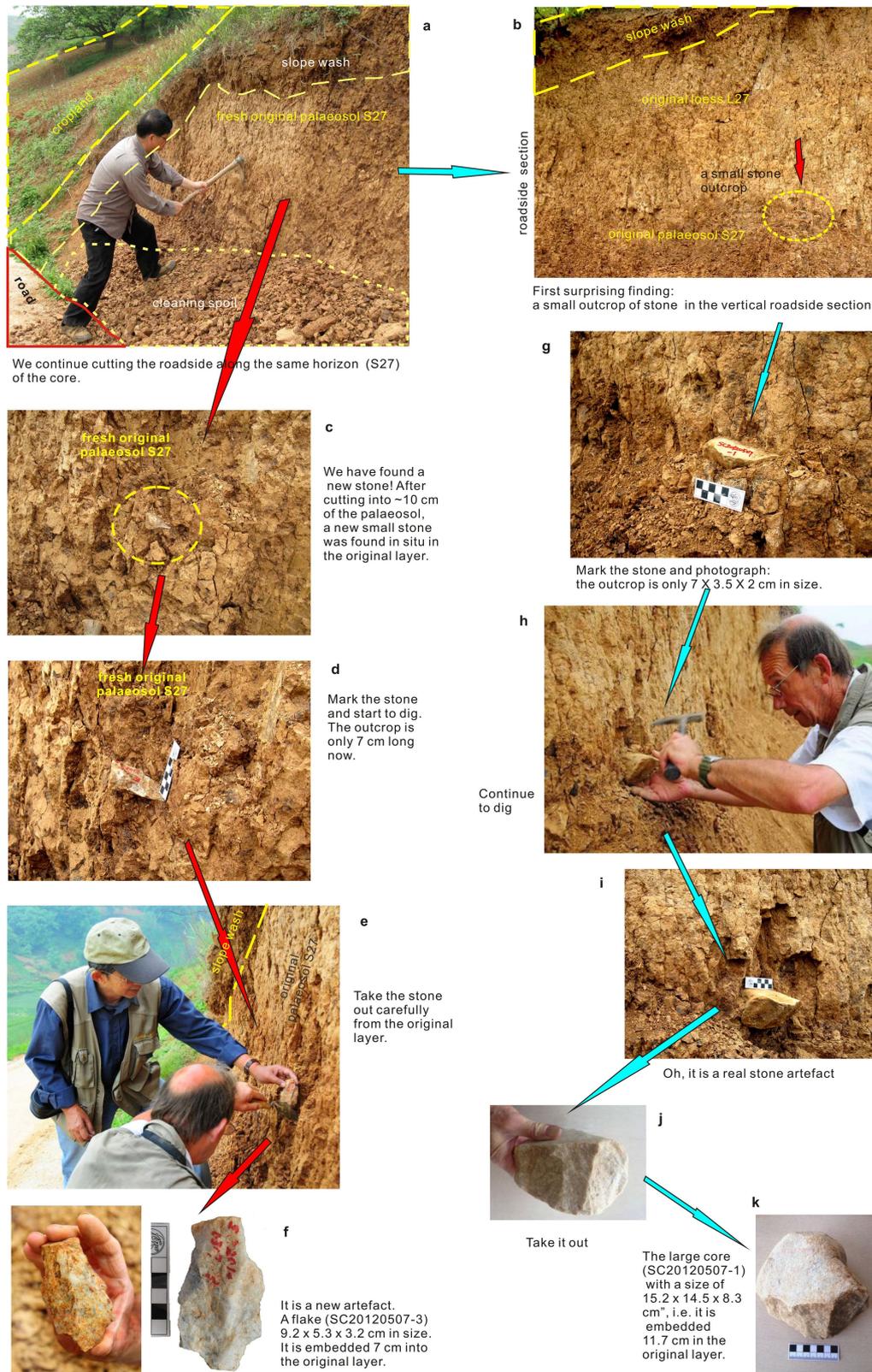
Extended Data Fig. 6 | See next page for caption.

**Extended Data Fig. 6 | Stone artefacts found during the sampling of S22 (1.54–1.57 Ma) and S24 (1.71–1.73 Ma) at the Shangchen section.** **a**, First discovery of a stone artefact in S22 ('place I'). **b**, Schematic profile of the section-cutting of place II. **c**, The place II section was excavated into the original palaeosol layer to a depth of about 150 cm. Note the presence of stone artefacts on a ledge in the original palaeosol, below the weathered crust. **d**, View of the excavation in subsection V. **e**, Profile of the original slope surface with a weathered crust of only 3–6-cm thickness, and no slope wash. Palaeomagnetic analysis of the samples taken around the stone artefacts confirmed that they were in undisturbed deposit. **f**, View of the excavation in S24. Note the weathered surface crust upslope, the slope wash to the left of the cutting and section cleaning debris below the excavation. **g**, Schematic profile of excavation into S24. **h**, Side view of place I of the section cut by the excavation, showing two artefacts within fresh original palaeosol. Note that there is a clear difference between the thin weathered crust and the original loess. **i–k**, Discovery and exposure of a large quartzite core in place II of the section (**i**, **j**), which led to the removal of the core shown in **k**. Details of the large core (SC080710-1) are given in Supplementary Table 6. Analysis of the palaeomagnetic samples taken alongside the stone artefacts showed that the loess and palaeosol was undisturbed, and did not represent slope wash.

a We continue cutting the roadside along the same horizon (S27) of the core.

b First surprising finding: a small outcrop of stone in the vertical roadside section.

c We have found a new stone! After cutting into ~10 cm of the palaeosol, a new small stone was found in situ in the original layer.

d Mark the stone and start to dig. The outcrop is only 7 cm long now.

e Take the stone out carefully from the original layer.

f It is a new artefact. A flake (SC20120507-3) 9.2 x 5.3 x 3.2 cm in size. It is embedded 7 cm into the original layer.

g Mark the stone and photograph: the outcrop is only 7 X 3.5 X 2 cm in size.

h Continue to dig

i Oh, it is a real stone artefact

j Take it out

k The large core (SC20120507-1) with a size of 15.2 x 14.5 x 8.3 cm", i.e. it is embedded 11.7 cm in the original layer.

Extended Data Fig. 7 | Details of artefacts excavated from the roadside section at the Shangchen locality from S27, which occurs below the Olduvai subchron and is dated to approximately 2.1 Ma. The hill slope is covered by a dark brown slope wash of 10–30-cm thickness that is easily distinguishable from the in situ loess in the roadside section. After cleaning the section, stone artefacts were exposed between 1.5 and 3 m below the top of the section, and extracted from in situ loess. **a**, **b**, This shows the obvious difference between slope wash and the original loess–palaeosol layer. **b**, First finding of a stone standing out of the surface crust which is situated about 1.5 m below the top of slope wash. **c–f**, The finding and collecting process for the artefact is the same in Extended Data Fig. 6. Details of the artefact SC 20120507-3—which was found after digging >30 cm into the fresh original palaeosol layer—are given in Fig. 4a, Supplementary Tables 6, 7 and Supplementary Video 1. **g–i**, A stone is marked with its specimen number before removal (**g**), and the artefact is disclosed step by step (**h**, **i**). **j**, The stone artefact after removal. **k**, View of core (SC20120507-1). Clear flake scars are evident. This piece is shown in Fig. 4d and details are given in Supplementary Tables 6, 7.
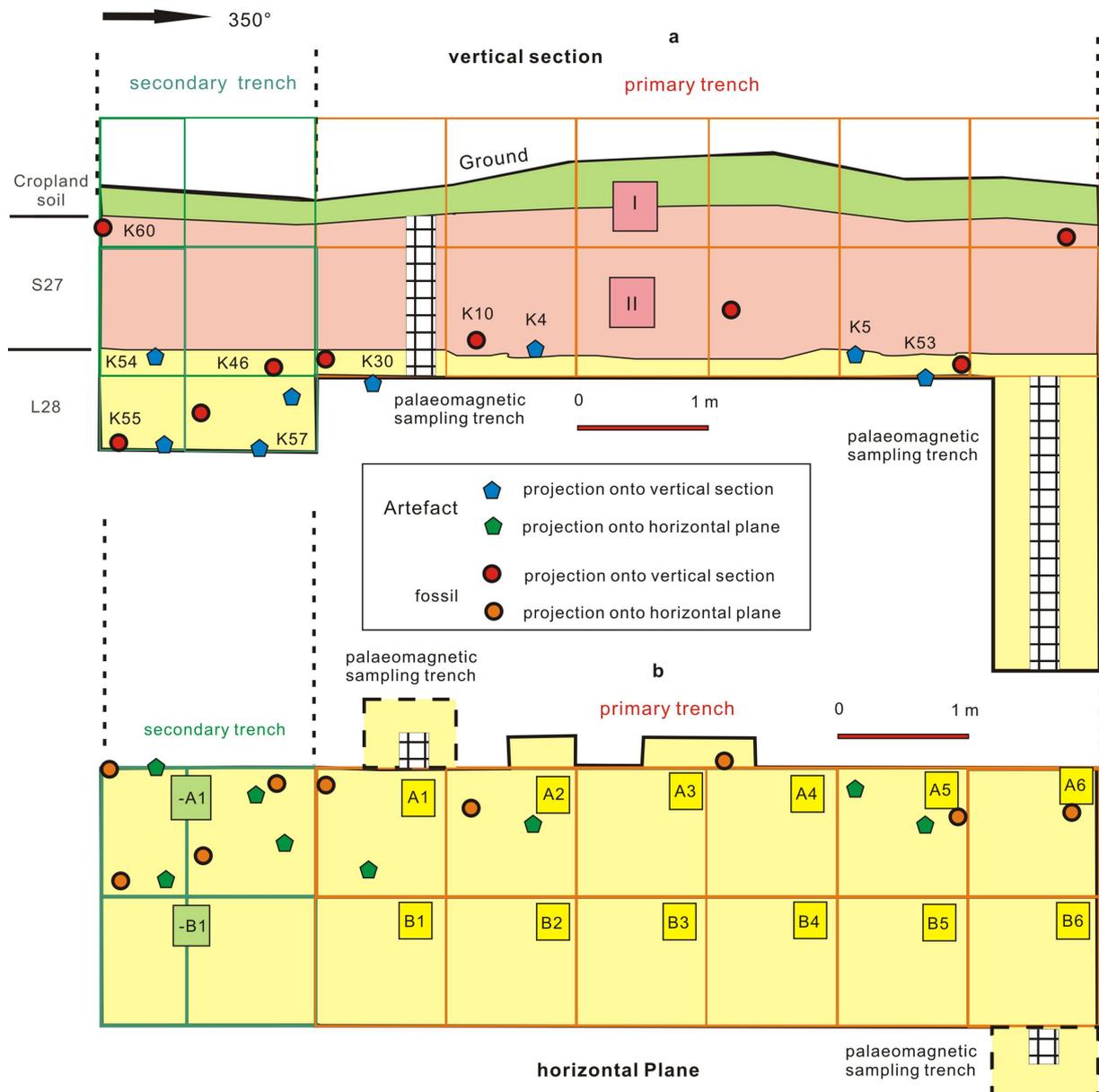
Extended Data Fig. 8 | The stratigraphic partition, grid layout and distribution of artefacts and fossils in the exploratory trench (subsection KW) in S27 and L28. a, b, The vertical section (**a**) and the horizontal plane (**b**) of the exploratory trench, which is composed of a primary and a secondary trench. The primary exploratory trench is 6 m long, 1.4–1.78 m deep and 2 m wide, and the secondary trench is 1.7 m long, 2 m deep and 2 m wide. The excavated area (approximately 15.4 m²) was divided into a grid of 1-m × 1-m squares. I, II, the numbers of grid lines on the vertical section. A1–A6 and B1–B6, numbers of the grid squares on the horizontal plane in the primary trench. –A1, –B1, the numbers of grid lines on the horizontal plane in the secondary trench. In the south and the north of the primary trench, 108 palaeomagnetic samples were continuously collected in two sampling trenches. The north sampling trench is 0.8–1 m wide and 2.3 m deep, and the south sampling trench is 0.4 m wide and 1.2 m deep. Some stone artefacts and fossil remains were excavated in situ in S27 and L28 from our exploratory trench. The features of eight artefacts can be seen in Fig. 4, Extended Data Fig. 10 and Supplementary Table 6. The fossils from the excavation were primarily tooth and bone fragments (Extended Data Fig. 10) of different animals, including a cervid, a bovid and a suid. No bones or jaws were complete. The fossil remains and stone artefacts occurred on the same horizon and were close to one another. Note that the artefacts and fossils also occur in the deepest part of the trench and not near the modern slope surface.
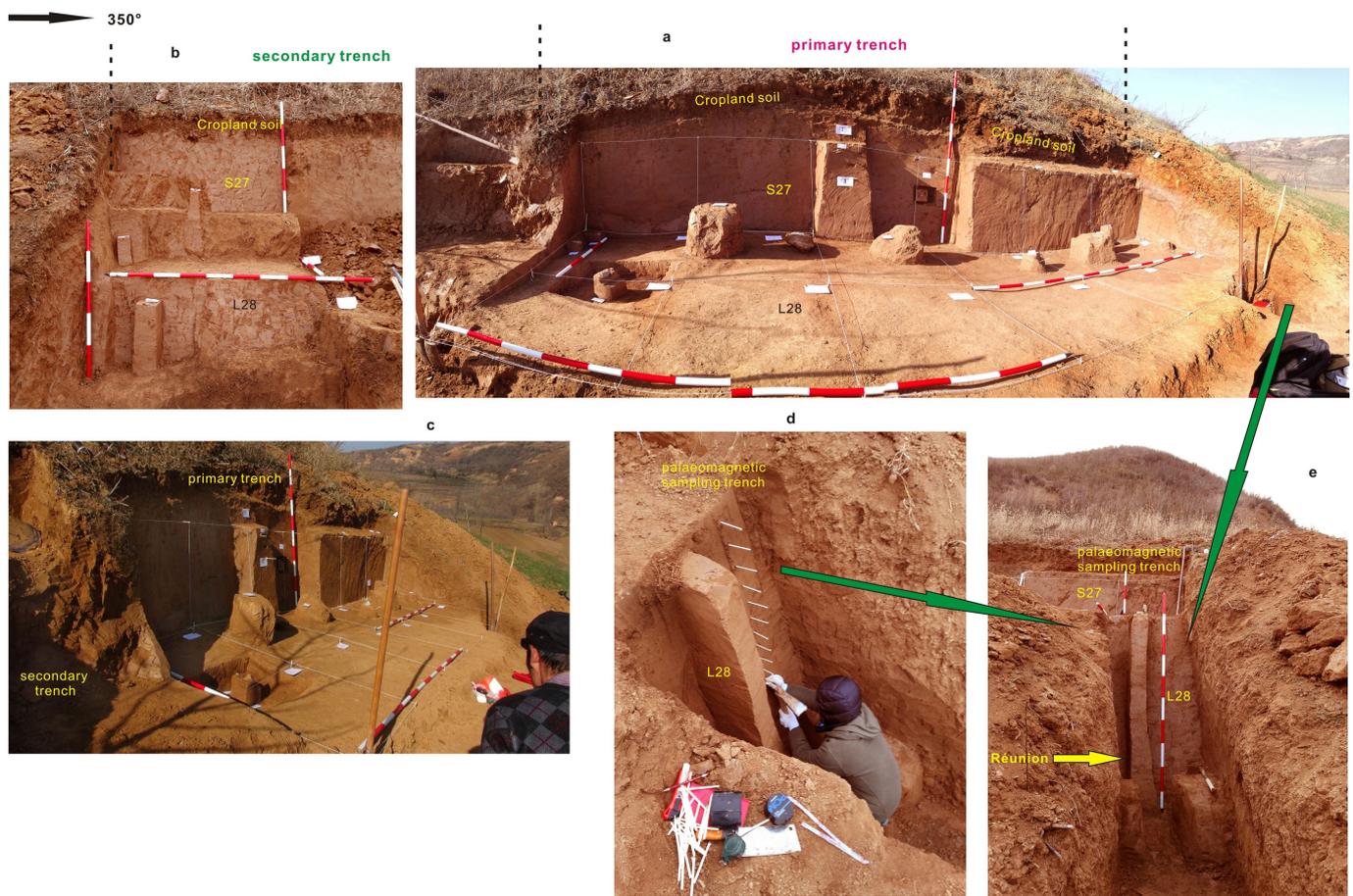
Extended Data Fig. 9 | The excavation of the exploratory trench (the subsection KW) in layers S27 and L28 at Shangchen locality. a–c, The primary (a, c) and secondary (b) exploratory trenches. d, e, Palaeomagnetic sampling trench in the north of the primary exploratory trench. The boundary between the cultivated horizon (cropland soil) and original loess horizon (S27) is very clear. The top layer is a grass-covered cropland soil of a depth of 20–40 cm (without any crops planted at this time). Underlying the cultivated layer are clear, homogeneous, solid and undisturbed loess–palaeosol strata. Several stones and fossils were found in situ in the original palaeosol–loess strata (S27–L28). These stones and mammalian fossils were kept in the reserved pillars of palaeosol and loess during the exploration process (a–c). The Réunion excursion is situated in the lower part (L28) of the palaeomagnetic sampling trench (e).
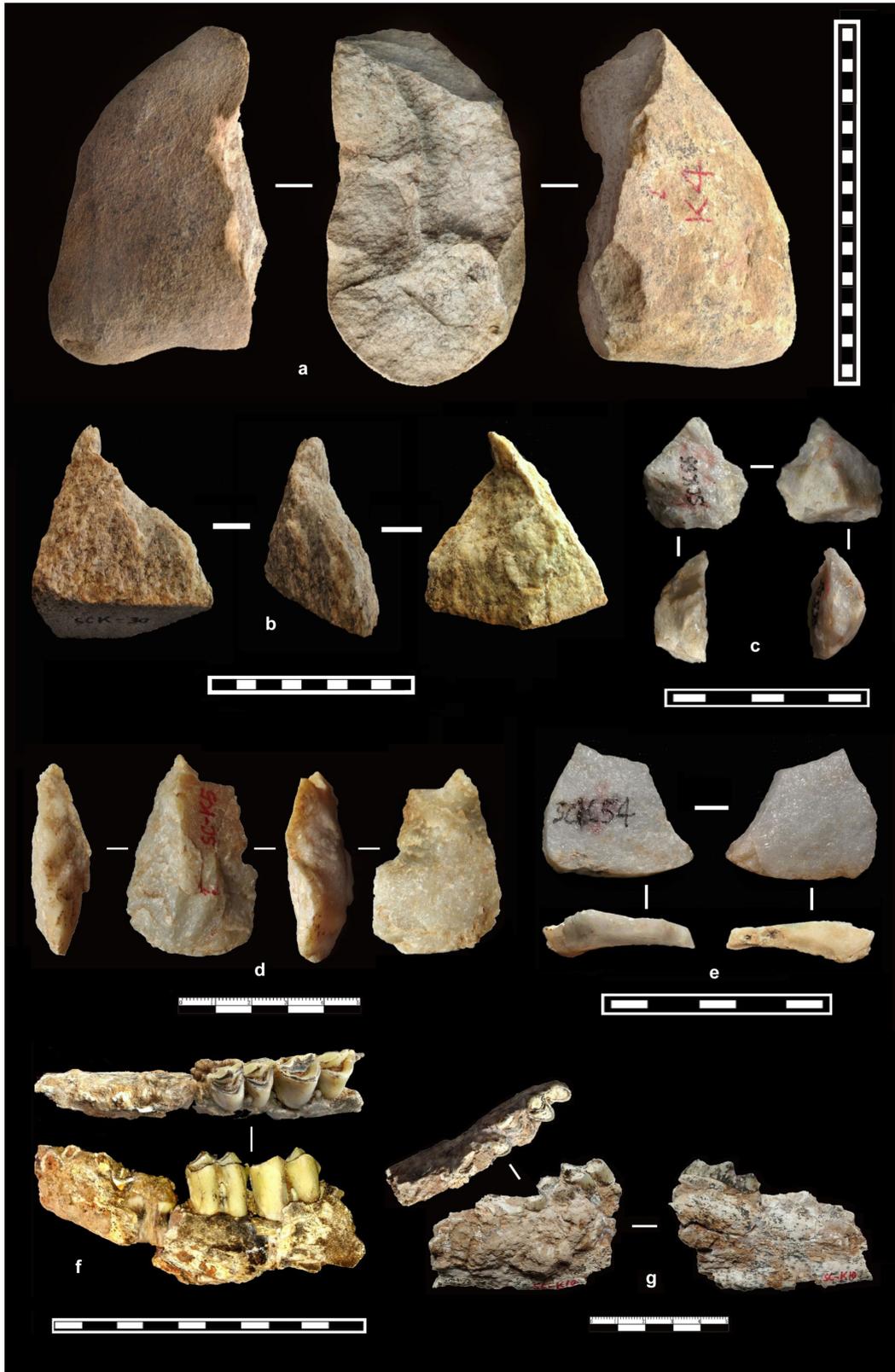
Extended Data Fig. 10 | See next page for caption.

Extended Data Fig. 10 | Selected artefacts and fossils from the exploratory trench (subsection KW) in S27 and L28. These are the oldest artefacts discovered at the Shangchen locality during this investigation. **a**, Quartzite core (SC-K4) from the boundary between S27 and L28 at a depth of 60–70 cm below the boundary between cultivated soil and fresh original palaeosol, and 164 cm above the end of the Réunion excursion. See Fig. 4i and Supplementary Tables 6, 7 for details. **b**, **c**, The oldest artefacts SC-K30 and SC-K55 within L28 from the exploratory trench, from 69–114 cm above the end of the Réunion excursion. See Supplementary Table 6 for details. **d**, Quartzite flake tool (SC-K5) from the exploratory trench, from the boundary between S27 and L28 at a depth of about 75 cm below the boundary between cultivated soil and fresh original palaeosol and 149 cm above the end of the Réunion excursion. See Fig. 4h and Supplementary Tables 6, 7 for details. **e**, Flake tool SC-K54 from within the L28 from the exploratory trench. **f**, Mandibular fragment of a small bovid (SC-K60) from the same horizon of S27 as the stone artefacts found during the excavation of S27 and L28. Top image shows the occlusal view of the mandible. **g**, A left mandibular fragment of a large cervid (SC-K10), which was found near and in the same horizon of S27–L28 as the stone artefacts SC-K4 and SC-K5. In the scales, each division represents 1 cm.

nature research

Corresponding author(s):   Zhaoyu Zhu, Robin Dennell

Reporting Summary

Nature Research wishes to improve the reproducibility of the work that we publish. This form provides structure for consistency and transparency in reporting. For further information on Nature Research policies, see Authors & Referees and the Editorial Policy Checklist.

Statistical parameters

When statistical analyses are reported, confirm that the following items are present in the relevant location (e.g. figure legend, table legend, main text, or Methods section).

n/a	Confirmed	
☐	☒	The exact sample size (*n*) for each experimental group/condition, given as a discrete number and unit of measurement
☐	☒	An indication of whether measurements were taken from distinct samples or whether the same sample was measured repeatedly
☐	☒	The statistical test(s) used AND whether they are one- or two-sided *Only common tests should be described solely by name; describe more complex techniques in the Methods section.*
☒	☐	A description of all covariates tested
☒	☐	A description of any assumptions or corrections, such as tests of normality and adjustment for multiple comparisons
☒	☐	A full description of the statistics including central tendency (e.g. means) or other basic estimates (e.g. regression coefficient) AND variation (e.g. standard deviation) or associated estimates of uncertainty (e.g. confidence intervals)
☒	☐	For null hypothesis testing, the test statistic (e.g. F, t, r) with confidence intervals, effect sizes, degrees of freedom and P value noted *Give P values as exact values whenever suitable.*
☒	☐	For Bayesian analysis, information on the choice of priors and Markov chain Monte Carlo settings
☒	☐	For hierarchical and complex designs, identification of the appropriate level for tests and full reporting of outcomes
☒	☐	Estimates of effect sizes (e.g. Cohen's *d*, Pearson's *r*), indicating how they were calculated
☒	☐	Clearly defined error bars *State explicitly what error bars represent (e.g. SD, SE, CI)*

Our web collection on statistics for biologists may be useful.

Software and code

Policy information about availability of computer code

Data collection	Mastersizer 2000 (version 5.61) was used to collect grain size data, Safyr (version SAFYR 7) was used to collect AMS data. VFTB control (version 4.0.009) was used to collect M-T and hysteretic loops data, and 2 G Enterprises Data Analysis was used to collect palaeomagnetic data.
Data analysis	Anisoft (version 4.2) was used to analyze the AMS data, and PaleoMag (version V3.1 b1) was used to analyze the palaeomagnetic data.

For manuscripts utilizing custom algorithms or software that are central to the research but not yet described in published literature, software must be made available to editors/reviewers upon request. We strongly encourage code deposition in a community repository (e.g. GitHub). See the Nature Research guidelines for submitting code & software for further information.

Data

> The authors declare that all the data supporting the findings of this study are available within the paper (and its supplementary information files). Source data for Figure 3 of the main text are also provided with the paper.

Field-specific reporting

Please select the best fit for your research. If you are not sure, read the appropriate sections before making your selection.

☐ Life sciences ☐ Behavioural & social sciences ☒ Ecological, evolutionary & environmental sciences

For a reference copy of the document with all sections, see [nature.com/authors/policies/ReportingSummary-flat.pdf](#)

Ecological, evolutionary & environmental sciences study design

All studies must disclose on these points even when the disclosure is negative.

Study description	Not applicable.
Research sample	Not applicable.
Sampling strategy	Not applicable.
Data collection	Not applicable.
Timing and spatial scale	Not applicable.
Data exclusions	Not applicable.
Reproducibility	Not applicable.
Randomization	Not applicable.
Blinding	Not applicable.

Did the study involve field work? ☒ Yes ☐ No

Field work, collection and transport

Field conditions	Field work was carried out in the Lantian area (Shaanxi Province, China), which lies on the southern margin of the Chinese Loess Plateau.
Location	Shangchen (SC) (34°13′33″N, 109°28′39″E), Lantian, Shaanxi Province, China.
Access and import/export	Palaeomagnetic samples and stone artefacts were collected with the help of the local residents.
Disturbance	Our excavations were conducted in an abandoned cropland, and the sediments were backfilled in the trench after our excavations

Reporting for specific materials, systems and methods

Materials & experimental systems

n/a	Involved in the study
☒	☐ Unique biological materials
☒	☐ Antibodies
☒	☐ Eukaryotic cell lines
☐	☒ Palaeontology
☒	☐ Animals and other organisms
☒	☐ Human research participants

Methods

n/a	Involved in the study
☒	☐ ChIP-seq
☒	☐ Flow cytometry
☒	☐ MRI-based neuroimaging

Palaeontology

Specimen provenance	A mandibular fragment of a cervid, a bovid and other fossil bone fragments were excavated from the loess sediments.
Specimen deposition	Some of the fossils are deposited in GIG, CAS, and others are deposited in IVPP, CAS.
Dating methods	Palaeomagnetism, Chiloparts and sedimentation rate dating.

☒ Tick this box to confirm that the raw and calibrated dates are available in the paper or in Supplementary Information.